Elasto-Plastic Behavior of Steel Pipe Beam-Column subjected to Cyclic Horizontal and Torsional Loads

by

Minoru SHUGYO*, JianPing LI* and Nobuo OKA***

The inelastic behavior of cantilever column with circular hollow section subjected to repeated proportional loading of horizontal and torsional loads under a constant axial compression is studied. An accurate numerical method for steel space frames and members with closed thin walled section which was developed by the authors is used to investigate the behavior. It is shown that a nonstationary characteristics, increase of out-of-plane deformation, is observed even in the column without an axial compressive load and a strong axial compressive load causes a significant divergence of out-of-plane deformation.

1. INTRODUCTION

Restoring force characteristics of a beam-column subjected to cyclic loadings are basic and very important factors in plastic design of building frames. Many investigations concerned with the inelastic behaviors of beam-columns under repeated biaxial bending and constant axial compression have been done so far[1,2] and it is well known that some interesting characteristics different from those under monotonic loading are observed. However, the effect of torsional moment was ignored in those papers. A large torsional moment can arise by a small torsional deformation in the member with colsed thin-walled section. Some factors which cause structure and member to twist are in a space bulding frame, e. g., eccentricity of the gravitational center, therefore, it is desirable to clarify the influence of torsional moment on the cyclic inelastic behaviors of the beam-column with closed thin-walled section.

In this paper the behavior of cantilever column with circular hollow section subjected to repeated proportional loading of horizontal and torsional loads in addition to a constant axial compressive load is investigated. The effect of torsion on the inelastic behavior is considered in the fiber level using von Mises yield criterion.

2. CANTILEVER COLUMN AND NUMERICAL METHOD

The analyzed cantilever column is shown in Fig. 1 with the global coordinate system (X, Y, Z). In the figure, L is the hight of the column, P, H_y, H_z and T are axial compressive, horizontal and torsional loads

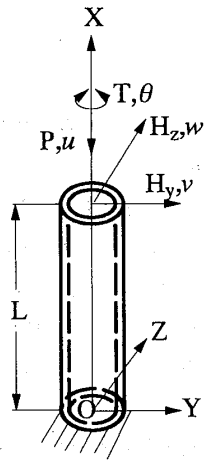

Fig. 1 Cantilever column

Received on May 7, 1996

*Dept. of Structural Engineering, Faculty of Engineering
**Dept. of Structural Engineering, Faculty of Engineering
***Japan Steel Tower Co., Ltd.

applied to the column top respectively, u, v, w and θ are the corresponding displacements. The numerical analysis is done by using a new method for geometrically and materially nonlinear analysis of steel member with closed thin walled section. The method is an advanced finite element method[3]. The column is divided into a number of elements along the length.

2.1 Geometrically nonlinear stiffness matrix

Member coordinate system(x, y, z)are shown in Fig. 2 . Utilizing an energy principle we can obtain the following equation:

$$d\boldsymbol{Q}=\boldsymbol{K}^e d\boldsymbol{q}^e \tag{1}$$

in which $\boldsymbol{K}^e$ is the geomertrically nonlinear tangent stiffness matrix and $\boldsymbol{Q}$ and $\boldsymbol{q}^e$ are nodal forces and nodal elastic displacements of an element, respectively. Both $\boldsymbol{Q}$ and $\boldsymbol{q}^e$ have 12 components.

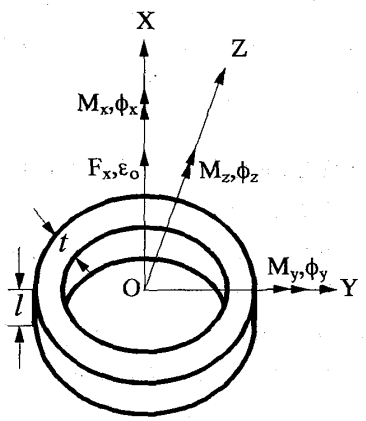

Fig. 2 Generalized stresses and strains of an element

2.2 Plastic tangent coefficient matrix for a cross section

In the present method, plastic deformation increment is estimated utilizing tangent coefficient matrix for a cross section. The tangent coefficient matrix is obtained by numerical integration of tangent stiffnesses of fibers which compose the element.

2.2.1 Incremental stress-strain relationship of a fiber

Assuming that only axial stress and shear stress due to St. Venant torsion participate in yielding of a fiber, the von Mises yield condition can be written as follows:

$$f(\sigma_{ij})=\sigma^2+3\tau^2-\sigma_y^2=0 \tag{2}$$

where σ is a normal stress due to axial force and bending moments, τ is a shear stress due to St. Venant torsion, and σ_y is the yield stress of a fiber. Denoting the translation of the center of the yield surface by α_{ij}, the subsequent yield condition which behaves according to Ziegler's modified kinematic hardening rule is represented as follows:

$$f(\sigma_{ij},\alpha_{ij})=0 \tag{3}$$

The flow rule is represented as

$$d\varepsilon_{ij}^p=\frac{\partial f(\sigma_{ij},\alpha_{ij})}{\partial\sigma_{ij}}d\lambda \tag{4}$$

where $d\varepsilon_{ij}^p$ is the increment of plastic strain, and $d\lambda$ is a positive scalar quantity. The elastic strain increments $d\varepsilon_{ij}^p$ are related to the stress increments $d\sigma_{ij}$ through Hooke's law, hence the incremental total stress-strain relation of a fiber is expressed as

$$\begin{Bmatrix}d\sigma\\ d\tau\end{Bmatrix}=\begin{bmatrix}D_{11} & D_{12}\\ D_{21} & D_{22}\end{bmatrix}\begin{Bmatrix}d\varepsilon\\ d\gamma\end{Bmatrix}\equiv\boldsymbol{D}^p\begin{Bmatrix}d\varepsilon\\ d\gamma\end{Bmatrix} \tag{5}$$

2.2.2 Plastic tangent coefficient matrix

The components of generalized stress vector $\boldsymbol{F}$ and generalized strain vector $\boldsymbol{\Delta}$ are shown in Fig. 2 . The components of $\boldsymbol{F}$ and $\boldsymbol{\Delta}$ can be written as

$$\left.\begin{aligned}\boldsymbol{F}&=[F_x\ M_x\ M_y\ M_z\ ]^T\\ \boldsymbol{\Delta}&=[\varepsilon_0\ \phi_x\ \phi_y\ \phi_z]^T\end{aligned}\right\} \tag{6}$$

where F_x is an axial force, M_x is a torsional moment, M_y and M_z are bending moments, and the components of $\boldsymbol{\Delta}$ are corresponding generalized strains, respectively. The increments of generalized stresses are related to the stress increments by

$$\left.\begin{aligned}dF_x&=\int d\sigma dA \quad dM_x=\int d\tau R dA\\ dM_y&=\int d\sigma z dA \quad dM_z=-\int d\sigma y dA\end{aligned}\right\} \tag{7}$$

while the strain increments are related to the increments of generalized strains by

$$\left.\begin{aligned}d\varepsilon&=d\varepsilon_0+z d\phi_y-y d\phi_z\\ d\gamma&=R d\phi_x\end{aligned}\right\} \tag{8}$$

where R is the distance from the centroid of the cross section to the center of the member wall. Substituting equations (5) and (8) into equation (7), we obtain the in-

cremental generalized stress-generalized strain relationship:

$$d\boldsymbol{F}=\boldsymbol{s}d\boldsymbol{\Delta} \tag{9}$$

where $\boldsymbol{s}$ is a tangent coefficient matrix. Let $\boldsymbol{s}^e$ denote an elastic tangent coefficient matrix and let $d\boldsymbol{\Delta}^e$ and $d\boldsymbol{\Delta}^p$ denote the elastic and plastic components of $d\boldsymbol{\Delta}$, respectively, then

$$\left.\begin{aligned} d\boldsymbol{F}&=\boldsymbol{s}^e d\boldsymbol{\Delta}^e \\ d\boldsymbol{\Delta}&=d\boldsymbol{\Delta}^e+d\boldsymbol{\Delta}^p \end{aligned}\right\} \tag{10}$$

Substituting equation (9) into (10) yields

$$d\boldsymbol{\Delta}^p=(\boldsymbol{s}^{-1}-\boldsymbol{s}^{e-1})\ d\boldsymbol{F}\equiv\boldsymbol{s}'d\boldsymbol{F} \tag{11}$$

where $\boldsymbol{s}'$ is a plastic tangent coefficient matrix. The elastic tangent coefficient matrix $\boldsymbol{s}^e$ is constant for any state of the section. The components of the tangent coefficient matrix can be obtained by numerical integration. In the present analysis an element is partitioned into 240 fibers. The stress and the tangent stiffness in each fiber are obtained as the average values at its centroid

2.3 Elastic-plastic tangent stiffness matrix

The following assumptions are made concerning the mechaninal behavior of the yielded element:

1) Plastic deformations consist of only four components that correspond to axial force, biaxial bending moments, and torsional moment.
2) Cross section does not distort.
3) An actual generalized plastic strain in a short element shown in Fig. 2 generally distributes nonlinearly. It is idealized with generalized plastic strains distributing linearly with the values at the element nodes i and j[3].
4) Incremental plastic deformations in the two $l/2$ portions occur concentrically at the element nodes i and j, respectively, where l is the length of the element.

Now let us define plastic displacement increments $d\boldsymbol{q}_i^p$, $d\boldsymbol{q}_j^p$ as

$$\left.\begin{aligned} d\boldsymbol{q}_i^p&=[du_i^p\ \ 0\ \ 0\ \ d\theta_{xi}^p\ d\theta_{yi}^p\ d\theta_{zi}^p]^T \\ d\boldsymbol{q}_j^p&=[du_j^p\ \ 0\ \ 0\ \ d\theta_{xj}^p\ d\theta_{yj}^p\ d\theta_{zj}^p]^T \end{aligned}\right\} \tag{12}$$

which are the nodal displacement increments due to the generalized plastic strain increments of an element. These plastic displacement increments can be obtained as described below.

The generalized stresses at the element nodes are obtained by the nodal forces with their coordinate transformation. Using these generalized stresses we can obtain the plastic tangent coefficient matrices $\boldsymbol{s}_i'$ and $\boldsymbol{s}_j'$ utilizing the procedure explained in the preceding section. Representing the components of $\boldsymbol{s}_i'$ by $(s'_{kl})_i$, a new square matrix $\boldsymbol{s}_i^p$ of 6 th order can be obtained as follows:

$$\boldsymbol{s}_i^p=\begin{bmatrix} (s'_{11})_i & 0 & 0 & (s'_{12})_i & (s'_{13})_i & (s'_{14})_i \\ 0 & 0 & 0 & 0 & 0 & 0 \\ 0 & 0 & 0 & 0 & 0 & 0 \\ (s'_{21})_i & 0 & 0 & (s'_{22})_i & (s'_{23})_i & (s'_{24})_i \\ (s'_{31})_i & 0 & 0 & (s'_{32})_i & (s'_{33})_i & (s'_{34})_i \\ (s'_{41})_i & 0 & 0 & (s'_{42})_i & (s'_{43})_i & (s'_{44})_i \end{bmatrix} \tag{13}$$

Another new matrix $\boldsymbol{s}_j^p$ which corresponds to $\boldsymbol{s}_j'$ can be obtained similarly. From assumptions 3) and 4) the plastic displacement increments can be obtained by the following equation:

$$\begin{Bmatrix} d\boldsymbol{q}_i^p \\ d\boldsymbol{q}_j^p \end{Bmatrix}=\frac{l}{8}\begin{bmatrix} 3\boldsymbol{s}_i^p & -\boldsymbol{s}_j^p \\ -\boldsymbol{s}_i^p & 3\boldsymbol{s}_j^p \end{bmatrix}\begin{Bmatrix} d\boldsymbol{Q}_i \\ d\boldsymbol{Q}_j \end{Bmatrix}\equiv\boldsymbol{s}^p\begin{Bmatrix} d\boldsymbol{Q}_i \\ d\boldsymbol{Q}_j \end{Bmatrix} \tag{14}$$

Since the total displacement increments $d\boldsymbol{q}$ are the sum of the elastic components $d\boldsymbol{q}^e$ and the plastic components $d\boldsymbol{q}^p$, an elasto-plastic tangent stiffiness matrix $\boldsymbol{K}^p$ is obtained as follows:

$$d\boldsymbol{Q}+\boldsymbol{R}=[I+\boldsymbol{K}^e\boldsymbol{s}^p]^{-1}\boldsymbol{K}^e d\boldsymbol{q}\equiv\boldsymbol{K}^p d\boldsymbol{q} \tag{15}$$

where $\boldsymbol{R}$ is the unbalanced force vector and $\boldsymbol{I}$ is the unit matrix.

The numerical analysis is carried out by a displacement control method[4] using $\boldsymbol{K}^p$. Coordinate transformation matrix of an element is updated and rigid body displacements are separated in each step by using orientation matrix[5].

3. NUMERICAL RESULTS AND DISCUSSION

The proposed method was applied to the analysis of a cantilever column with hollow circular section. Sizes and mechanical properties of the column are as follows: outside diameter of the cross section D is 10.0 cm, thickness t is 0.40cm, hight of the column L is 63.1cm, Young's modulus E is 2.06×10^5MPa, yield

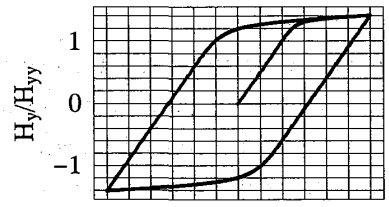

$H_y/H_{yy}\sim v/v_y$ curve

Fig.3 Load-displscement hysteresis curve ($P/P_y=0$, $v_a=3\,v_y$)

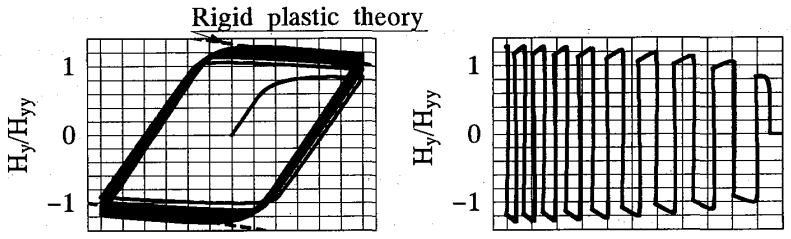

(a) $H_y/H_{yy}\sim v/v_y$ curve (b) $H_y/H_{yy}\sim u/u_y$ curve

Fig.4 Load-displacement hysteresis curves ($P/P_y=0.5$, $v_a=3\,v_y$)

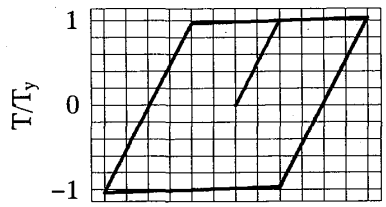

$T/T_y\sim\theta/\theta_y$ curve

Fig.5 Load-displacement hysteresis curve ($P/P_y=0$, $\theta_a=3\,\theta_y$)

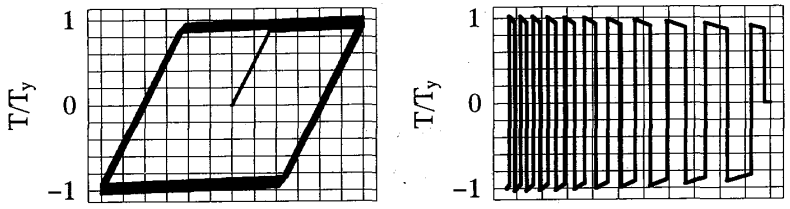

(a) $T/T_y\sim\theta/\theta_y$ curve (b) $T/T_y\sim u/u_y$ curve

Fig.6 Load-displacement hysteresis curves ($P/P_y=0.5$, $\theta_a=3\,\theta_y$)

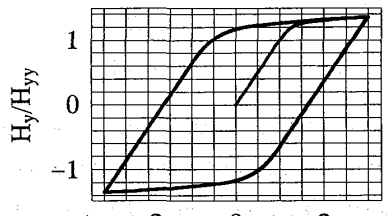

(a) $H_y/H_{yy}\sim v/v_y$ curve

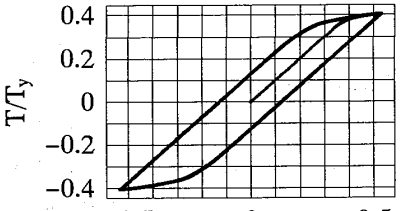

(b) $T/T_y\sim\theta/\theta_y$ curve

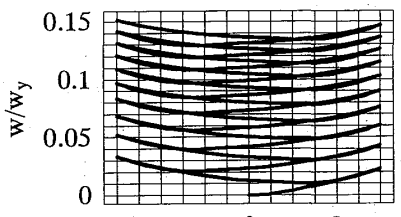

(c) Displacement orbit at the top of the column

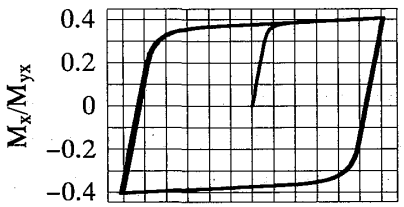

(d) $M_x/M_{yx}\sim\phi_x/\phi_{yx}$ curve

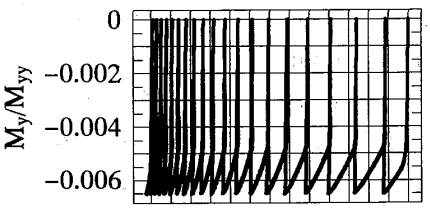

(e) $M_y/M_{yy}\sim\phi_y/\phi_{yy}$ curve

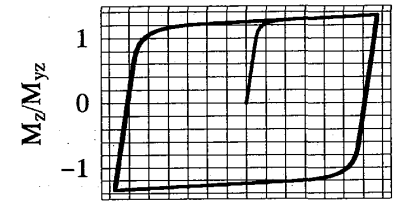

(f) $M_z/M_{yz}\sim\phi_z/\phi_{yz}$ curve

Fig.7 Load-displacement hysteresis curves and generalized stress-strain relationships at the bottom section ($P/P_y=0$, $(T/T_y)/(H_y/H_{yy})=0.3$, $v_a=3\,v_y$)

stress σ_y is 235.0 MPa, and strain hardening modulus after yielding H is $E/100$. The nondimensionalized slenderness ratio λ of the column is 0.4. λ was defined by the equation $\lambda=2L\sqrt{\varepsilon_y}/\pi r$, where ε_y is yield strain of material and r is radius of gyration about principal axis of the section.

The results are plotted by nondimensionalized values. The basic values used to nondimensionalze are as follows: initial yield values of axial compressive, horizontal and torsional loads at the column top P_y, H_{yy}, H_{yz} and T_y, the corresponding initial yield displacements u_y, $u_y(=w_y)$, θ_y, initial yield torsional

and bending moments M_{yx}, M_{yy} and M_{yz}, the corresponding initial yield generalized strains ϕ_{yx}, ϕ_{yy} and ϕ_{yz}. The column was divided into 20 elements of equal length. Initial imperfections and initial residual strains were not considered.

Figures 3 and 4 show the behaviors for 10 cycles repeated horizontal load under the constant axial compressive loads $P/P_y=0.0$ and $P/P_y=0.5$, respectively. The analyses were done by controlling the displacement amplitude at the column top v_a as $v_a=3v_y$. The results show the similar tendency reported in a previous paper[1] concerned with the cyclic behaviors of a column of strain hardening material: resisting moment does not increase by a cyclic loading in case of $P/P_y=0.0$, while hysteresis loop of moment-curvature curve approaches gradually to that for $P/P_y=0.0$ and also an accumulation of average axial strain occurs when an axial compressive load exists. Figures 5 and 6 are the results for 10 cycles repeated torsional moment under the constant axial compressive loads $P/P_y=0.0$ and $P/P_y=0.5$, respectively. The analyses were done by controlling the amplitude of rotation angle at the column top θ_a as $\theta_a=3\theta_y$. The characteristics are similar to those for horizontal load except that the accumulation of axial displacement becomes larger since the whole column yields.

The load-displacement hysteresis curves, displacement orbit at the top of the column and the generalized stress-generalized strain curves at the bottom cross section of the column for 10 cycles repeated proportional loading of $(T/T_{yy})/(H_y/H_{yy})=0.3$ are shown in Fig. 7. It looks like a stable response from Figs. 7 (a) and 7 (b), however, an out-of-plane displacement w occurs and increases gradually with the increase of the

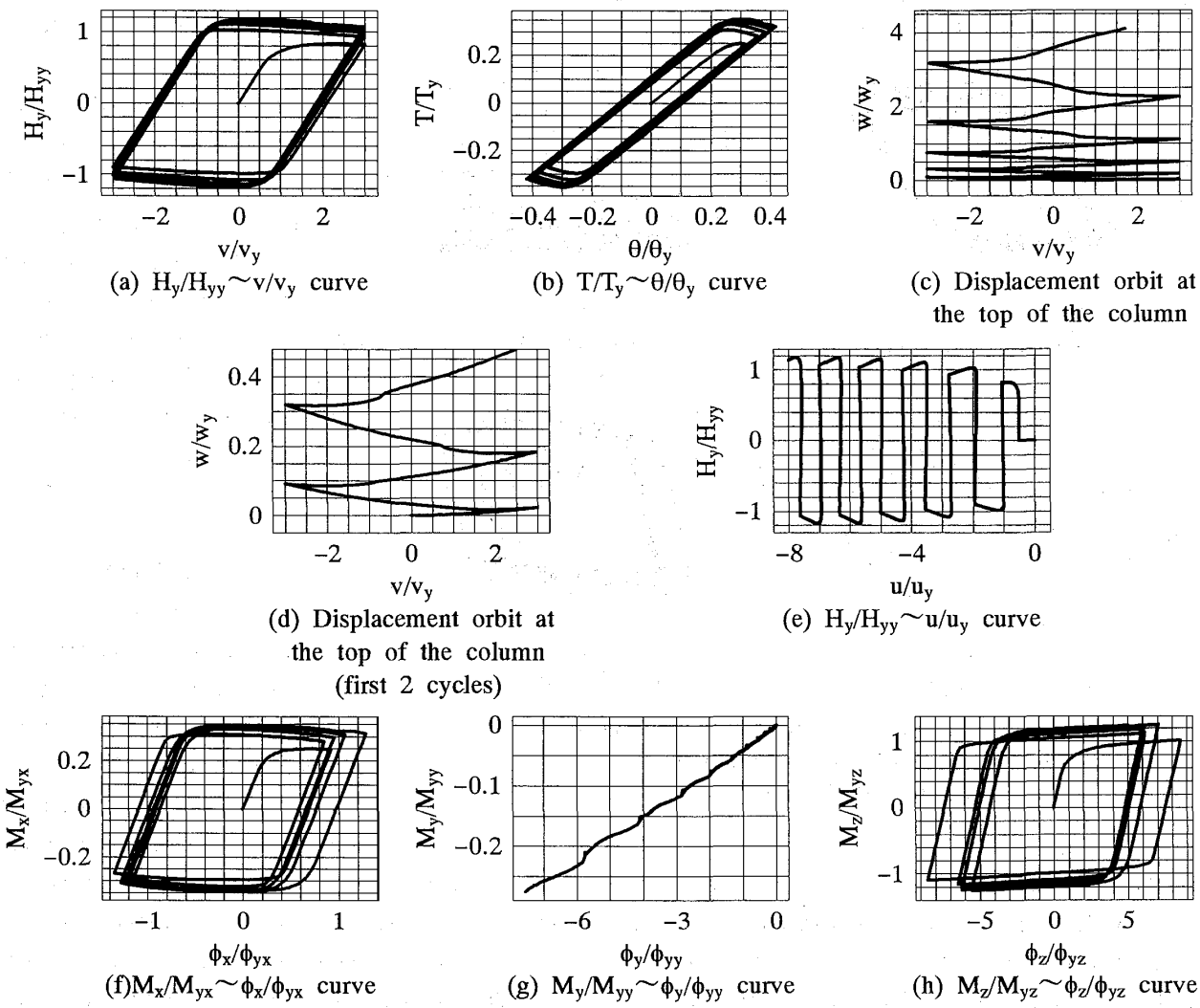

(a) $H_y/H_{yy}\sim v/v_y$ curve (b) $T/T_y\sim\theta/\theta_y$ curve (c) Displacement orbit at the top of the column

(d) Displacement orbit at the top of the column (first 2 cycles) (e) $H_y/H_{yy}\sim u/u_y$ curve

(f) $M_x/M_{yx}\sim\phi_x/\phi_{yx}$ curve (g) $M_y/M_{yy}\sim\phi_y/\phi_{yy}$ curve (h) $M_z/M_{yz}\sim\phi_z/\phi_{yz}$ curve

Fig.8 Load-displacement hysteresis curves and generalized stress-strain relationships at the bottom section ($P/P_y=0.5$, $(T/T_y)/(H_y/H_{yy})=0.3$, $v_a=3v_y$)

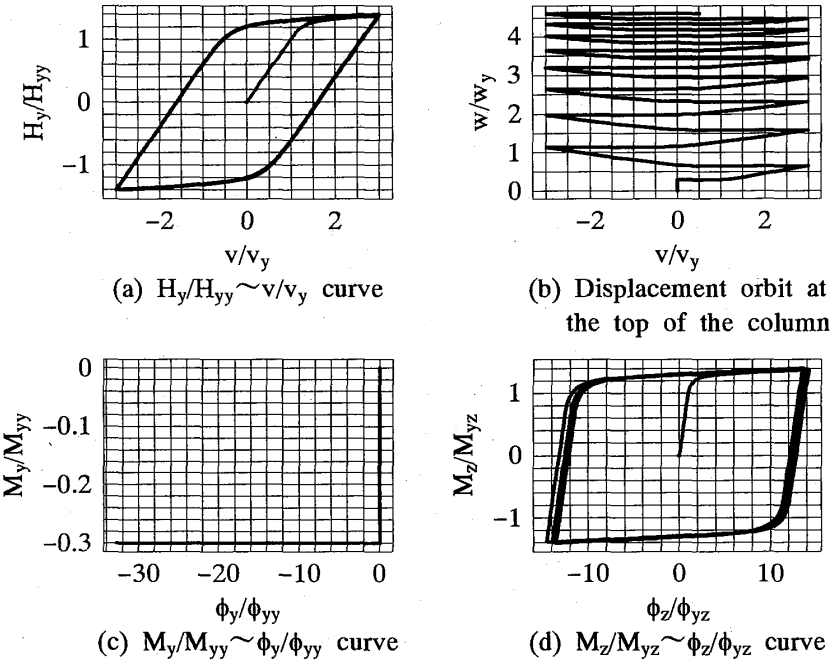

(a) $H_y/H_{yy}\sim v/v_y$ curve (b) Displacement orbit at the top of the column

(c) $M_y/M_{yy}\sim\phi_y/\phi_{yy}$ curve (d) $M_z/M_{yz}\sim\phi_z/\phi_{yz}$ curve

Fig. 9 Load-displacement hysteresis curves and generalized stress-strain relationships at the bottom section ($P/P_y=0$, $H_z/H_{yz}=0.3$, $v_a=3v_y$)

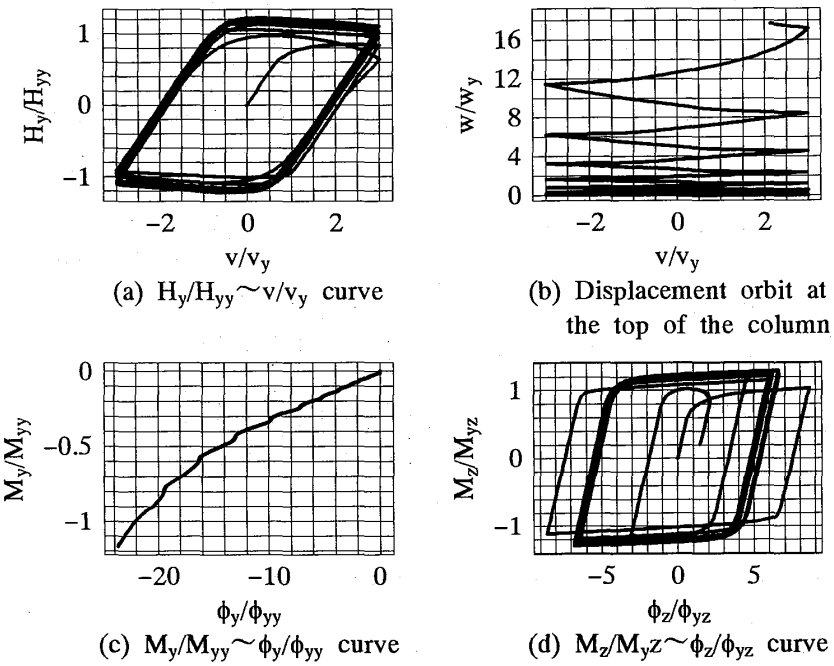

(a) $H_y/H_{yy}\sim v/v_y$ curve (b) Displacement orbit at the top of the column

(c) $M_y/M_{yy}\sim\phi_y/\phi_{yy}$ curve (d) $M_z/M_yz\sim\phi_z/\phi_{yz}$ curve

Fig. 10 Load-displacement hysteresis curves and generalized stress-strain relationships at the bottom section ($P/P_y=0.5$, $H_z/H_{yz}=0.01$, $v_a=3v_y$)

number of repetition as seen in Fig. 7 (c). The out-of-plane displacement is due to the accumulation of the residual curvature about Y-axis at the bottom section of the column (Fig. 7 (e)) . This phenomena suggests that the column may collapse in out-of-plane direction under an axial compressive load since an accumulation of out-of-plane displacement is observed even in the column without an axial load. Figure 8 shows the results for 10 cycles repeated loading of $(T/T_{yy})/(H_y/H_{yy})=0.3$ under the constant axial load $P/P_y=0.5$. The out-of-plane displacement diverges vigorously from the beginning of the loading and the column is going to collapse.

Fig. 9 and 10 are the results for repeated loading of H_y with a constant initial load H_z under the constant axial loads $P/P_y=0$ and $P/P_y=0.5$, respectively. The figures show that an out-of-plane constant load is very dangerous for the beam-column subjected to repeated horizontal loading and the effect of the out-of-plane constant load is almost similar to that of the proportionally loaded torsional load.

Therefore it can be said that the out-of-plane load secondarily caused by the column top deflection and the torsional load is the reason of the divergence of out-of-plane deformation of the beam-column subjected to repeated proportional loading of horizontal and torsional loads.

4. CONCLUSIONS

The inelastic behavior of cantilever column with circular hollow section subjected to repeated proportional loading of horizontal and torsional loads in addition to a constant axial compressive load was studied. The following conclusions can be drawn from the aforementioned numerical examples. (1)An accumulation of out-of-plane deformation is observed even for zero axial compressive load. The deformation has a tendency to approach gradually to a certain value. (2)Hence a strong axial compressive load may cause a significant divergence of

out-of-plane deformation. (3) The divergence of out-of-plane deformetion is caused by the secondary effect of the column top deflection and the torsional load.

REFERENCES

[1] Igarashi, S., Matui, C., Yoshimura, K. and Matsumura, K.: Inelastic Behaviours of Structural Steel Sections under Alternative Loadings Part (1) and Part (2), Trans. A. I. J., No. 169, pp. 53−62, 1970 and No. 170, pp. 39−50, 1970.

[2] Uetani, K., Nakamura, T.: Symmetry Limit Theory for Cantilever Beam Column subjected to Cyclic Reversed Bending, J. Mech. Phys. Solids, Vol. 31, No. 6, pp. 449−484, 1983.

[3] Shugyo, M., Li, JianPing and Oka, Nobuo: Inelastic and Stability Analysis of Linearly Tapered Box Columns under Biaxial Bending and Torshion, Reports of Faculity of Engneering, Nagasaki University, No. 43, pp. 143−149, 1995.

[4] Ramm, E.: The Riks/Wempner Approach-An Extension of the Displacement Control Method in Nonlinear Analysis, Recent Advances in Nonlinear Computational Mechanics, Pineridge Press, 1982.

[5] Yoshida, Y., Masuda, N., Morimoto, T., and Hirosawa, N.: An Incremental Formulation for Computer Analysis of Space Framed Structures, Proc. JSCE, No. 300, pp. 21−31, 1980 (in Japanese).